

Lawrence Berkeley National Laboratory

Recent Work

Title

NEUTRINO MASS LIMITS FROM THE $K^0 \rightarrow \pi^+ e^- \bar{\nu}_e$ DECAY SPECTRA

Permalink

<https://escholarship.org/uc/item/0sr702jv>

Authors

Clark, Alan R.

Elioff, T.

Frisch, H.J.

et al.

Publication Date

1973-09-01

c.1

NEUTRINO MASS LIMITS FROM THE $K_L^0 \rightarrow \pi^\pm l \bar{\nu}$
DECAY SPECTRA

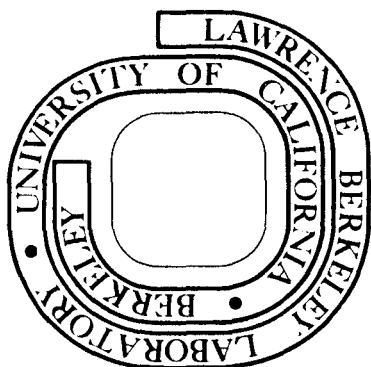
Alan R. Clark, T. Elioff, H. J. Frisch,
Rolland P. Johnson, Leroy T. Kerth, G. Shen, and W. A. Wenzel

September 1973

Prepared for the U. S. Atomic Energy Commission
under Contract W-7405-ENG-48

For Reference

Not to be taken from this room



DISCLAIMER

This document was prepared as an account of work sponsored by the United States Government. While this document is believed to contain correct information, neither the United States Government nor any agency thereof, nor the Regents of the University of California, nor any of their employees, makes any warranty, express or implied, or assumes any legal responsibility for the accuracy, completeness, or usefulness of any information, apparatus, product, or process disclosed, or represents that its use would not infringe privately owned rights. Reference herein to any specific commercial product, process, or service by its trade name, trademark, manufacturer, or otherwise, does not necessarily constitute or imply its endorsement, recommendation, or favoring by the United States Government or any agency thereof, or the Regents of the University of California. The views and opinions of authors expressed herein do not necessarily state or reflect those of the United States Government or any agency thereof or the Regents of the University of California.

NEUTRINO MASS LIMITS FROM THE $K_L^0 \rightarrow \pi^\pm \ell^\mp \bar{\nu}$
DECAY SPECTRA*

Alan R. Clark, T. Elioff, H. J. Frisch**
Rolland P. Johnson, Leroy T. Kerth, G. Shen, and W. A. Wenzel

Lawrence Berkeley Laboratory
University of California
Berkeley, California

ABSTRACT

A magnetic spectrometer at the Bevatron has been used to study the low neutrino energy ends of the $K_{\mu 3}$ and $K_{e 3}$ spectra. The spectra are found to agree well with the V-A predictions for massless neutrinos. The upper limits (90% C.L.) are 650 KeV for the muon neutrino mass and 450 KeV for the mass of the electron neutrino.

I. INTRODUCTION

The most precise limits on the muon neutrino mass have been set by measuring the energy¹ or momentum² of the muon in $\pi \rightarrow \mu \nu_\mu$ decays. While this method is straightforward, it is quite sensitive to the value of the pion mass. A determination of the muon neutrino mass is presented here which is practically independent of the uncertainty in the pion mass. The method used is to examine the low neutrino energy ends of the $K_L^0 \rightarrow \pi^+ \mu^+ \bar{\nu}$ ($K_{\mu 3}$) and $K_L^0 \rightarrow \pi^+ e^+ \bar{\nu}$ ($K_{e 3}$) spectra. As will be shown, the use of $K_L^0 \rightarrow \pi^+ \pi^-$ ($K_{\pi\pi}$) events for mass scale calibration decreases the sensitivity of the neutrino mass determinations to previously measured particle masses.

A comparison of the results and methods of muon neutrino mass determinations is shown in Table I. It should be noted that for all methods the quantity actually measured is the square of the rest mass; hence reducing the mass limit by one half involves an experiment which is four times as sensitive.

Also determined in this experiment is a limit on the mass of the electron neutrino. Very precise measurements³ of the positron spectrum from tritium beta decay have set limits on the electron neutrino mass of ~ 60 eV. The comparatively crude limits set by the present experiment (450 KeV) offer both a check on the experimental method for determination of the muon neutrino mass and a new limit on the mass of electron neutrinos from strangeness-changing decays. The latter result is significant when one considers the paucity of experimental evidence on the existence of different types of neutrinos.

In addition as a test of CPT invariance, the spectra for neutrinos are compared with the corresponding spectra for anti-neutrinos. Our limits on the mass differences are much more stringent than those implied by comparisons of π^+ and π^- lifetimes.

II. EXPERIMENTAL METHOD

1. General

The V-A theory of weak interactions predicts little dependence of the $K_{\ell 3}$ matrix element on the neutrino mass. However, the boundary of the Dalitz plot is modified for a non-zero neutrino mass.

In the present experiment the measured invariant mass $m_{\pi\ell}$ of the two charged secondaries is simply related to the neutrino energy in the kaon center of mass by

$$E_{\nu} = \frac{m_K^2 - m_{\pi\ell}^2 + m_{\nu}^2}{2m_K} \cong \frac{(m_K + m_{\pi\ell})}{2m_K} (m_K - m_{\pi\ell}) \cong m_K - m_{\pi\ell}.$$

Simultaneously detected $K_L^0 \rightarrow \pi^+ \pi^-$ ($K_{\pi\pi}$) decays are used to measure the resolution of the apparatus and calibrate the absolute invariant mass scale. Since the $K_{\pi\pi}$ events effectively measure the kaon mass, the present results are independent of previously measured values of the kaon mass. Since the neutrino energy depends only in second order on the pion mass, the uncertainty in the pion's mass (14 KeV) leads to an uncertainty of about 8 KeV in the neutrino energy measurement.

2. Apparatus

Figure 1 shows the plan view of the detection apparatus. The 6-m-long evacuated decay volume began 7.6 m from the production target in the Bevatron External Proton Beam. The 0.8-msr. beam yielded $\sim 6 \times 10^5$ K_L in the momentum range 0.8 - 3.2 GeV/c for 6×10^{11} protons on the target. The momenta of the decay secondaries were measured in symmetric spectrometers, each with a 0.9-m x 0.6-m aperture picture-frame magnet and five double gap magnetostrictive wire spark chambers. The chambers were designed with low mass (5.2×10^{-4} radiation lengths) and the volumes between the spark chambers were filled with helium to reduce Coulomb scattering.

Downstream of the last spark chamber on each side of the apparatus, counter hodoscopes F and R selected trajectories with maximum horizontal divergences of ± 45 mrad from the beam line. This angular requirement selected secondary particles emerging from the decay volume with transverse momenta within a rather narrow interval; the desired interval was selected by setting the magnet current appropriately. A six counter array H was mounted in front of each F hodoscope, and a large counter T for fast timing was mounted behind each R hodoscope.

Electrons were identified in 2.3 m long Freon Cherenkov counters, which were found to be more than 99.6% efficient during preliminary tests. Muons were identified by range measurements. The range detectors each contained a 1 m long carbon block followed by 17 cells of steel and scintillator. Each cell consisted of one or more 1.2 m x 1.2 m x 2.5 cm steel plates. The number of plates in each cell was chosen to give a muon range interval of approximately 7% for momenta between 0.5 and 1.6 GeV/c.

The data discussed here were accumulated as (useful) background during a search for the rare decay modes $K_L^0 \rightarrow \mu^+ \mu^-$, $e^+ e^-$ and $\mu^\pm e^\mp$ which has been previously reported^{4, 5}. The spectrometer magnets were set to correspond to a transverse momentum of 225 MeV/c, the center-of-mass momentum of the decay $K_L^0 \rightarrow \mu^+ \mu^-$. The trigger logic required a particle on each side which satisfied the angular requirement and also counted in the H array and the timing counter. Events with an electron which bent inward at angles between 15 and 45 mrad were rejected; this veto reduced the K_{e3} background in the dilepton sample at the expense of the data presented here. The signals from the Cherenkov counters (except as noted above) and the range counters were not used in the trigger but were recorded for use

later in the analysis. The signals from the counters and the spark chamber information for each event were accumulated, checked, and then stored on magnetic tape by a PDP-9 computer. Beam intensity and magnet currents were recorded each Bevatron pulse.

For the low neutrino energy (or high $m_{\pi\ell}$) region of the $K_{\ell 3}$ Dalitz plot the spark chamber trigger used for the rare decay mode search was ideal. By requiring both charged secondaries to have transverse momenta greater than 200 MeV/c, only those $K_{\ell 3}$ events of interest here were accumulated. The only significant background with respect to particle identification involved $K_L^0 \rightarrow \pi^+\pi^-$ decays in which a pion decayed upstream of the magnets and simulated a $K_{\mu 3}$ event. This background will be discussed in Section VII.

III. DATA SAMPLE.

The events were reconstructed and analyzed with a CDC-6600 computer. An event was considered a $K_{\mu 3}$ or $K_{e 3}$ candidate if the two reconstructed trajectories met within 2 cm in the decay volume and if the reconstructed angles and momenta were kinematically consistent with such a decay. Any particle accompanied by a Cherenkov count was assumed to be an electron; other particles were tried as pions and muons. Each event with no Cherenkov count was also considered as a possible $K_{\pi\pi}$ candidate if the vertex cut described above was satisfied and if the reconstructed parent particle originated at a point less than 4.0 cm from the production target.

For this first stage analysis, an effective-length parameterization of the magnetic fields was used. This simple procedure provided adequate mass resolution for the initial selection of events with a minimum expenditure of computer time. Better momentum resolution and discrimination against impossible trajectories could be achieved by a step-by-step integration of the trajectories through the measured magnetic fields. Accordingly,

for one out of five $K_{\pi\pi}$ events and for all $K_{\ell 3}$ events with $m_{\pi\ell}$ greater than 475 MeV (as determined from the first analysis), each charged secondary trajectory was numerically integrated using the measured magnetic field maps. Events with discontinuous trajectories, indicating a decay in flight or an error in spark association, were eliminated. The cuts were quite stringent and corresponded to about two standard deviations on each of eight parameters measuring deviations from orbit continuity. Approximately 60% of the data survived these cuts. The integrated trajectory was also used to correct the momentum estimate.

To be identified as a muon, a particle was required to stop within 1.5 counters of its expected range. This corresponds to requiring that the muon range be within about 10% of the expected value. A pion was identified by a range more than 1.5 counters short of the expected range of a muon of the same momentum. If both particles in an event satisfied the muon range criterion, the event was removed from the $K_{\mu 3}$ sample. The laboratory momenta of the secondary particles were determined primarily by the kaon laboratory momentum ($\langle P_K \rangle \approx 2.2 \text{ GeV}/c$) and only weakly correlated with the Dalitz plot position. Therefore, over the small invariant mass interval used for the neutrino mass determination, elimination of events with ambiguous π or μ identification did not bias the $K_{\mu 3}$ decay spectra.

Having determined the momenta and identities of the charged secondaries, one could calculate the invariant mass ($m_{\pi\ell}$) and the neutrino energy (E_ν) in the kaon rest frame. Events for which the reconstructed kaon could not have

originated within 5 cm of the production target were eliminated. This cut was purposely very loose because the calculation of the distance of closest approach of the parent kaon to the target is coupled to the invariant mass calculation. If the cut were too tight it could distort the shape of the spectrum. Scatter plot studies of $K_{\ell 3}$ data comparing the distance of closest approach to the target as a function of $m_{\pi\ell}$ indicated that no bona-fide events were lost by the kinematic compatibility requirement.

IV. APPARATUS RESOLUTION AND INVARIANT MASS CALIBRATION

Figure 2 is a semi-log plot of the $K_{\pi\pi}$ invariant mass distribution. The spectrum can be fitted quite well by a superposition of two Gaussian forms centered about the same mass plus a linear background. Changing the cut on the distance of closest approach to the target from 5 cm to 2 cm does not appreciably change the width of the $K_{\pi\pi}$ peak although the linear background does decrease. The wider Gaussian is compatible with $K_{\pi\pi}$ events in which a pion has decayed in flight or scattered from the material in the spark chambers while the linear background is compatible with $K_{\mu 3}$ events in which a muon has been misidentified as a pion. To eliminate as much of the $K_{\mu 3}$ contamination as possible, all $K_{\pi\pi}$ events with kaons which could not have originated within 2 cm of the production target were eliminated.

The invariant mass plot shown in figure 2 has been used as the resolution function of the apparatus. Although the resolution should be normally distributed as a function of the square of the invariant mass, the results of this experiment are insensitive to such details of the fitting procedure primarily

because the invariant mass intervals for the $K_{\ell 3}$ fits are small.

The tails of the distribution shown in figure 2 are from $K_{\mu 3}$ decays in which the neutrino direction is parallel to the kaon direction or from $K_{\pi\pi}$ events in which one pion has decayed in flight. For each of these two sources of broadening the measured width of the $K_{\pi\pi}$ peak is greater than the resolution width expected for $K_{\ell 3}$. (Note that there are two pions which can decay in flight for $K_{\pi\pi}$ as compared to one pion for $K_{\ell 3}$). For this experiment the tails of the $K_{\pi\pi}$ peak were small enough that they did not affect the fits appreciably. Furthermore, the use of a resolution function wider than that of the apparatus would lead to less stringent limits on the neutrino masses.

V. DETECTION EFFICIENCY

The detection efficiency of the apparatus was determined with a numerical integration scheme (the program LAS VEGAS) in which events were generated uniformly in phase space and traced through the apparatus. Figure 3 shows the $K_{\mu 3}$ detection efficiency and the V-A spectrum as a function of neutrino energy. The efficiency is normalized to unity at the zero neutrino energy end. The efficiency at 5 MeV neutrino energy drops by only 14% from the maximum at the tip.

The $K_{e 3}$ efficiency is further distorted because the Cherenkov counters were used in anticoincidence to reject events if the electron bent inward downstream of the magnets. Although this trigger scheme had little effect on the events at the tip of the Dalitz plot, it decreased the detection efficiency for $K_{e 3}$ events relative to that for $K_{\mu 3}$ events for lower values of $m_{\pi\ell}$.

VI. K_{e3} SPECTRA

Figure 4 shows the K_{e3} data compared to the V-A prediction for a zero mass neutrino, including the effect of resolution. A value of $\lambda_+ = .04$ is used for the K_{e3} form factor. The only adjustable parameter is the normalization. For the mass interval $485 < m_{\pi e} < 499$ MeV, the χ^2 is 19 for 27 degrees of freedom (C.L. $\sim 90\%$) and the data agree with the spectrum in the interval $475 < m_{\pi e} < 485$ MeV. The quality of the fit indicates that the V-A theory gives a good representation of the data and that the LAS VEGAS program is a good **representation** of the apparatus.

Shown in the Inset of figure 4 is the variation of χ^2 as a function of electron neutrino mass. The minimum is at 0 KeV and the corresponding 90% limit is 350 KeV where the χ^2 increases by 1.6. Since only the square of the neutrino mass enters into all relevant formulae, an excess of events at the tip of the spectrum would correspond to an imaginary neutrino mass. Unfortunately the necessary expressions cannot be analytically continued to imaginary masses (the V-A current-current interaction allows negative transition probabilities in such cases, for example) and fits for imaginary neutrino mass are model-dependent. Predicted spectra for imaginary masses were obtained by increasing the kaon's mass slightly in the calculation of the matrix element to keep the V-A helicity structure at the Dalitz plot boundaries. The Dalitz plot boundaries for the phase space part of the transition probability were calculated for imaginary masses. For this and other reasonable models the minimum remained at zero neutrino mass when imaginary masses were considered. The shape of the imaginary mass part of the χ^2 curve clearly depends on a particular

model, however, and so is not used in the determination of the errors on the mass limit. It should be noted that even if the χ^2 minimum were at an imaginary mass, we would still take the 90% limit as the mass where the χ^2 increased by 1.6 over the χ^2 at $m_\nu = 0$.

VII. $K_{\mu 3}$ SPECTRA

(1) $K_{\pi\pi}$ Background

Events from the decays $K_L \rightarrow \pi^+\pi^-$ are a significant background to the $K_{\mu 3}$ end point studies. In fact, approximately 10^6 $K_{\pi\pi}$ decays were detected during the course of the experiment; this is to be compared with approximately 10^4 $K_{\mu 3}$ decays with neutrino energies in the interval 0 to 5 MeV. Even a fraction of a percent of $K_{\pi\pi}$ events would cause background problems if identified as $K_{\mu 3}$. A pion from $K_{\pi\pi}$ which decayed upstream of the momentum analysis system, for example, would generally cause the event to be classified as a $K_{\mu 3}$ if the muon entered the range device.

Such mis-identified $K_{\pi\pi}$ events show up in the $m_{\pi\mu}$ spectrum as a rather broad peak near $m_{\pi\mu} \approx 480$ MeV. Figure 5 shows the apparent $m_{\pi\mu}$ distributions for a subset of the $K_{\pi\pi}$ events shown in Figure 2 with one secondary pion intentionally misidentified as a muon. Figure 6 shows the complete $K_{\mu 3}$ spectrum compared to the predicted V-A spectrum normalized to the uppermost 5 MeV in the mass spectrum. The $K_{\pi\pi}$ background is apparent.

(2) Fitting Procedure

To eliminate the $K_{\pi\pi}$ background in the $K_{\mu 3}$ spectrum, different intervals of $\pi\mu$ invariant mass were tried in order to find the extent of the background free region. Leaving the upper limit of the fitting interval fixed

at 499 MeV, the V-A fit for zero neutrino mass was tried using different lower limits. For all fitting intervals starting at or above 493 MeV the fits are acceptable, and have χ^2 probabilities which are stable and are similar to those of the K_{e3} events in the same mass interval. When fits with V-A for neutrino masses greater than 1.6 MeV were tried, no acceptable fits were possible for any mass interval.

As long as the ratio of the $K_{\pi\pi}$ background to the $K_{\mu 3}$ spectrum decreases monotonically as the neutrino energy decreases, any inclusion of this background will lead to neutrino mass limits which are too large. That is, the higher background at the lower end of the fitted interval, when used in the normalization, simulates a depletion of events at high $m_{\pi\mu}$ corresponding to a massive neutrino.

The $m_{\pi\mu}$ spectrum for the $K_{\mu 3}$ data is shown in Figure 7 along with fits for zero and 1.6 MeV neutrino mass. The inset shows the χ^2 distribution as a function of neutrino mass. The minimum is at zero mass with a $\chi^2 = 13.7$ for 10 degrees of freedom. The confidence level for the fit is about 20%. The χ^2 as a function of m_ν increases by 1.6 at about 550 KeV and that is taken as the limit (90% confidence level) for the neutrino mass.

A similar analysis was performed for the K_{e3} data in the $m_{\pi e}$ interval 493.5 to 499 MeV. The fitted results are shown in Figure 8 for zero and 1.6 MeV neutrino masses. The fit for zero mass is good ($\chi^2 = 9.2$ for 10 degrees of freedom; confidence level ~ 50%) although the 90% confidence level limit for the neutrino mass is only slightly worse (~ 400 KeV) than for the larger mass interval shown in Figure 4.

VIII. RESULTS AND CONCLUSIONS

(1) Systematic errors.

The overall normalization is affected by a number of parameters which have a negligible effect on the final neutrino mass limits. Examples are the K_{e3} form factors, the radiative corrections⁶ and uncertainties in the detection efficiency. In general, very large changes in the form factors or the radiative cut-off parameter of the detection efficiency drop-off cause the V-A fits to become slightly worse. However, even though the minimum χ^2 becomes worse, the position of the minimum does not change. This is because the effect of a massive neutrino is seen as a significant change in the shape of the spectrum only at the low E_ν end rather than a gradual shift in the data or a slight renormalization.

Two things to which the results are sensitive are the width of the mass resolution function and, for the $K_{\mu3}$ spectrum, the cuts on the muon range requirement. If the resolution function is made wider by allowing more background events in the $K_{\pi\pi}$ spectrum (Fig. 2), the quality of the fits for both the K_{e3} and $K_{\mu3}$ spectra deteriorate. When the muon range requirement is relaxed, $m_{\pi\mu}$ events are not fitted as well, presumably because more $K_{\pi\pi}$ background is included.

The 90% confidence levels on the neutrino mass limits vary over a range of about 100 KeV depending on the particular resolution function and muon range cut used. Including these systematic uncertainties, the overall limits are 650 KeV for the muon neutrino and 450 KeV for the electron neutrino (90% C.L.)

(2) Test of CPT Invariance

CPT Invariance implies equality of the neutrino and antineutrino masses. Since muons and electrons of both charge signs were accepted by the apparatus, the final data samples contain about equal mixtures of neutrinos and antineutrinos. The spectra for the neutrinos are found to be the same as those for the corresponding antineutrinos. The mass difference is less than 450 KeV (90%) between the electron neutrino and its antiparticle and between the muon neutrino and its antiparticle. The only other limit on a neutrino-antineutrino mass difference seems to be that implied by the limit on the difference in π^+ and π^- lifetimes.⁷

We wish to thank Dr. R. Clive Field for help during the first stages of the experiment and Dr. William R. Holley for many helpful discussions. Michael Barnes and John P. Wilson assisted thoughtfully during the data analysis and we gratefully acknowledge their participation.

REFERENCES

* Work done under the auspices of the United States Atomic Energy Commission.

** Present address: Enrico Fermi Institute of Physics, University of Chicago
Chicago, Illinois 60637

1. E. S. Shrum and K. O. H. Zlok, Phys. Letters 37B, 115 (1971).
2. P. S. L. Booth, R. G. Johnson, E. G. H. Williams and J. R. Wormald, Phys. Letters 26B, 39 (1967).
3. Karl-Erik Bergkvist, CERN 69-7, 91 (1969)
4. Alan R. Clark, T. Eloff, R. C. Field, H. J. Frisch, Rolland P. Johnson Leroy T. Kerth, and W. A. Wenzel, Phys. Rev. Letters 26, 1667 (1971).
5. H. J. Frisch, Thesis, UCRL-20264, 1971 (unpublished).
6. E. S. Ginsberg Phys. Rev. 171, 1675 (1968). Dr. Ginsberg kindly gave us copies of programs to calculate the relevant radiative corrections.
7. D. S. Ayres, A. M. Cormack, A. J. Greenberg, R. W. Kenney, D. O. Caldwell, V. B. Elings, W. P. Hesse, and R. J. Morrison, Phys. Rev. 3D, 1051 (1971). Using the V-A theory to calculate the dependence of the transition probability $\Gamma (\pi^{\pm} \rightarrow \mu^{\pm} \nu)$ on neutrino mass, the 90% C. L. limit on the difference between the muon neutrino and its antiparticle is found for that experiment to be ~ 4 MeV.

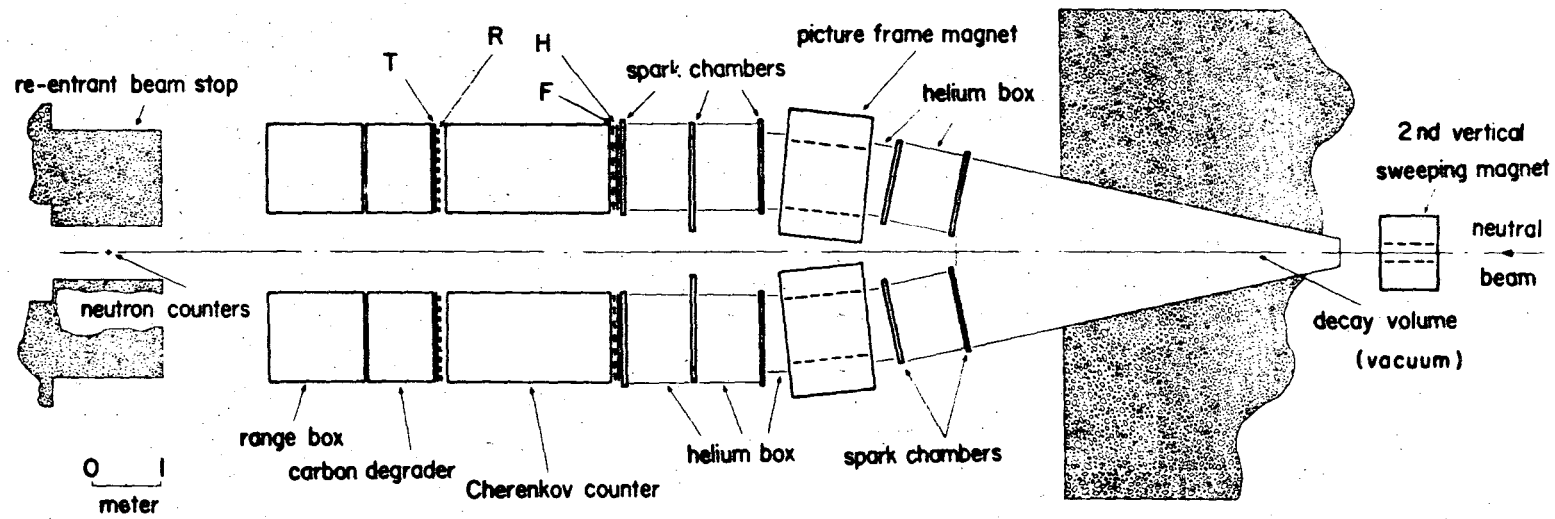
T A B L E I

MUON NEUTRINO MASS MEASUREMENTS

<u>Decay Mode</u>	<u>Limit (MeV)</u> <u>90% C.L.</u>	<u>Method</u>	<u>Reference</u>
$\pi^{\pm} \rightarrow \mu^{\pm} \nu$	3.6	Muon range in emulsion	Barkas (1956)
$\mu^{+} \rightarrow e^{+} \nu \nu$	1.5	Positron momentum measured with magnetic spectrometer	Peoples (1966)
$\pi^{\pm} \rightarrow \mu^{\pm} \nu$	2.2	Muon range in LH _e B.C.	Hyman (1967)
$\pi^{+} \rightarrow \mu^{+} \nu$	1.6	Muon momentum measured with magnetic spectrometer	Boothe (1967)
$\pi^{+} \rightarrow \mu^{+} \nu$	1.15	Muon energy with Ge(Li) detector	Shrum (1971)
$K_L^0 \rightarrow \pi^{\pm} \mu^{\mp} \nu$	0.65	$\pi\mu$ invariant mass with magnetic spectrometer	This Experiment

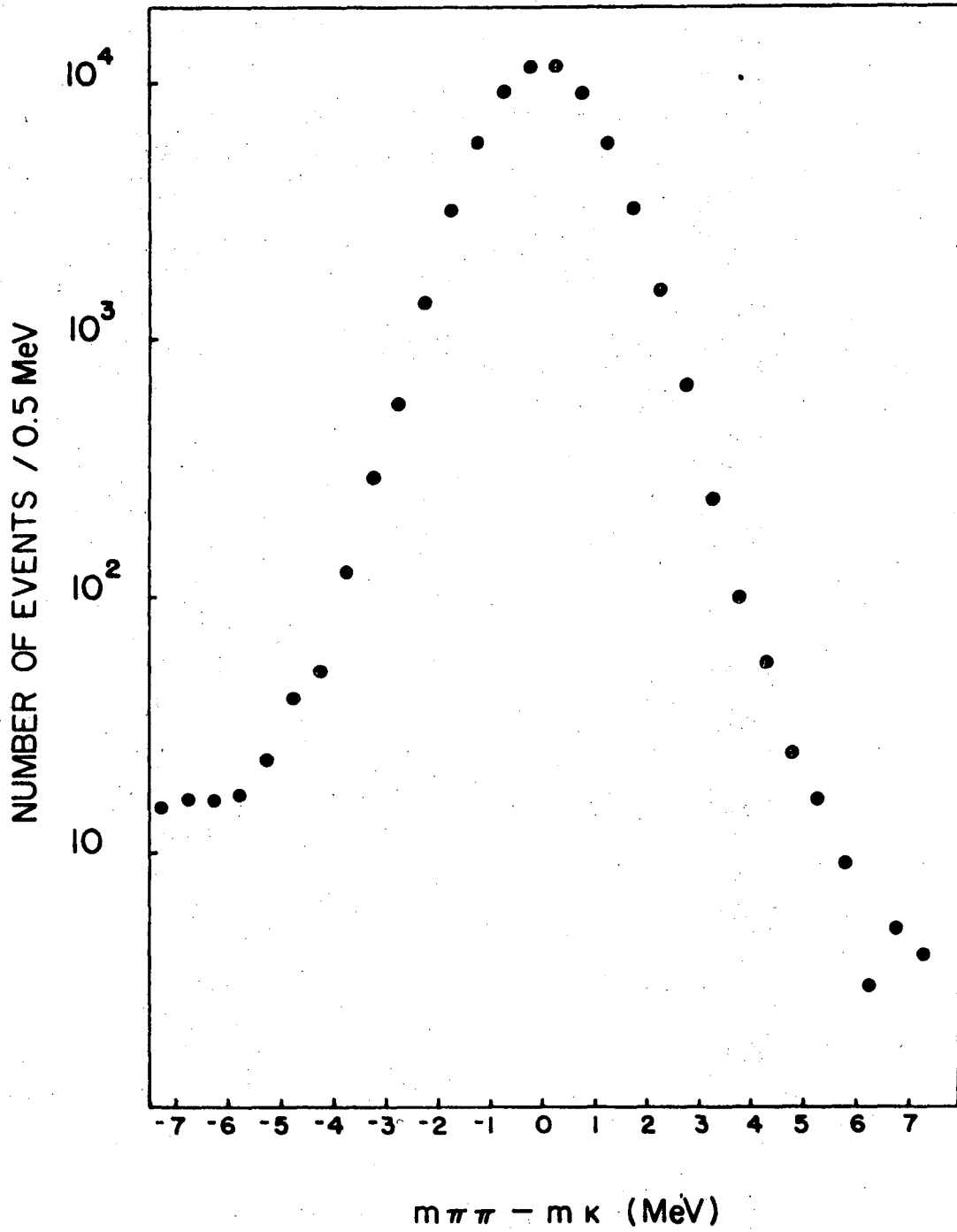
- (a) W. H. Barkas, W. Birnbaum and F. M. Smith, Phys. Rev. 101, 778 (1956).
- (b) J. Peoples, Nevis Laboratory Ph.D. Thesis R-457, CU-253, NEVIS-147 (1966), unpublished.
- (c) L. G. Hyman, J. Loken, E. G. Pawitt, M. Derrick, T. Fields, J. McKenzie, I. T. Wang J. Fetkovich, G. Keyes, Phys. Letters 25B, 376 (1967).
- (d) See Ref. 2
- (e) See Ref. 1

- Fig. 1. Plan view of the apparatus. F and R are counter hodoscopes. H is a six counter array. T is a fast timing counter.
- Fig. 2. Semi-log plot of the $\pi\pi$ invariant mass spectrum used as the resolution function of the apparatus and the absolute invariant mass scale calibration for the neutrino mass fits.
- Fig. 3. Detection efficiency of the apparatus compared with the theoretical V-A $K_{\mu 3}$ spectrum as a function of the neutrino center of mass energy. In the interval 0 to 5 MeV neutrino energy the detection efficiency changes only 14%.
- Fig. 4. The πe invariant mass spectrum compared with the theoretical V-A prediction with the detection efficiency and resolution included. The fitted interval is $485 < m_{\pi e} < 499$. The inset shows the χ^2 as a function of neutrino mass.
- Fig. 5. The $\pi\mu$ invariant mass spectrum found by purposely incorrectly identifying as a muon one of the pions from $K_{\pi\pi}$ decays. The vertical scale is expanded by a factor of 10 for $m_{\pi\mu} > 485$ MeV.
- Fig. 6. The $\pi\mu$ invariant mass spectrum from $K_{\mu 3}$ events compared with the theoretical V-A spectrum normalized to the interval $495 < m_{\pi\mu} < 500$ MeV. The background centered at 480 MeV is from incorrectly identified $K_{\pi\pi}$ decays.
- Fig. 7. The $\pi\mu$ invariant mass spectrum compared with the theoretical V-A prediction in the interval $493.5 < m_{\pi\mu} < 499$. The smooth (dashed) curve corresponds to $m_{\nu\mu} = 0.0$ (1.6) MeV. The inset shows the χ^2 as a function of neutrino mass.
- Fig. 8. The πe invariant mass spectrum compared with the theoretical V-A predictions for the same interval used in Fig. 7. The limit on the neutrino mass is only slightly worse than for the complete interval. The general character of the fits is similar to those in Fig. 7.



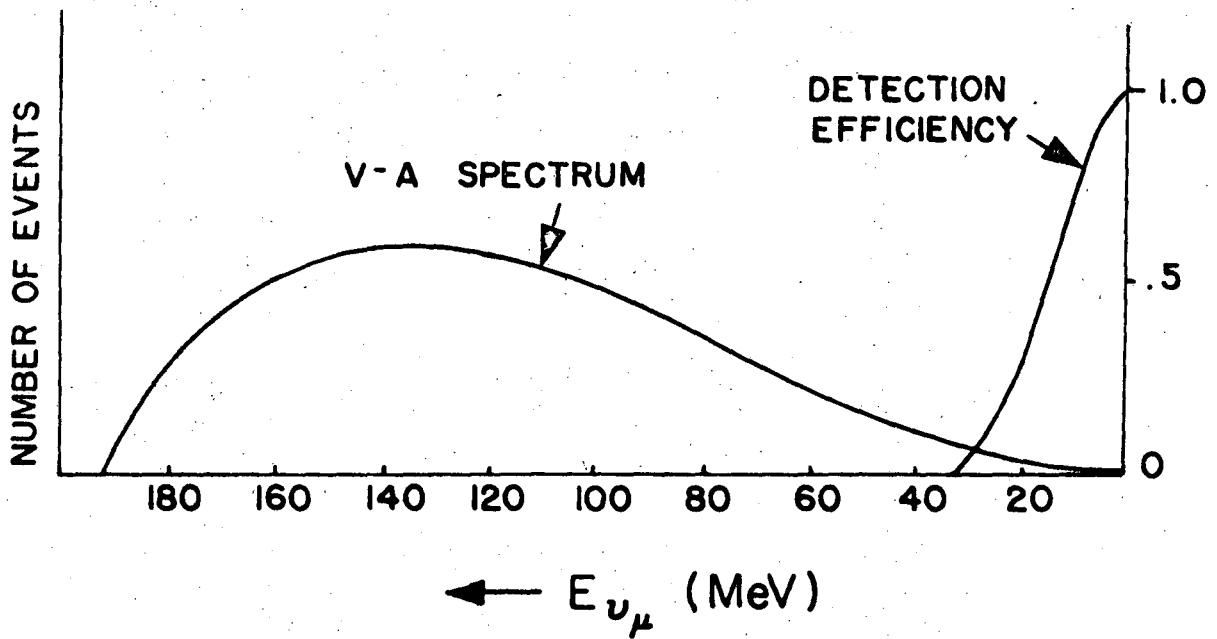
XBL 702-315

Fig. 1



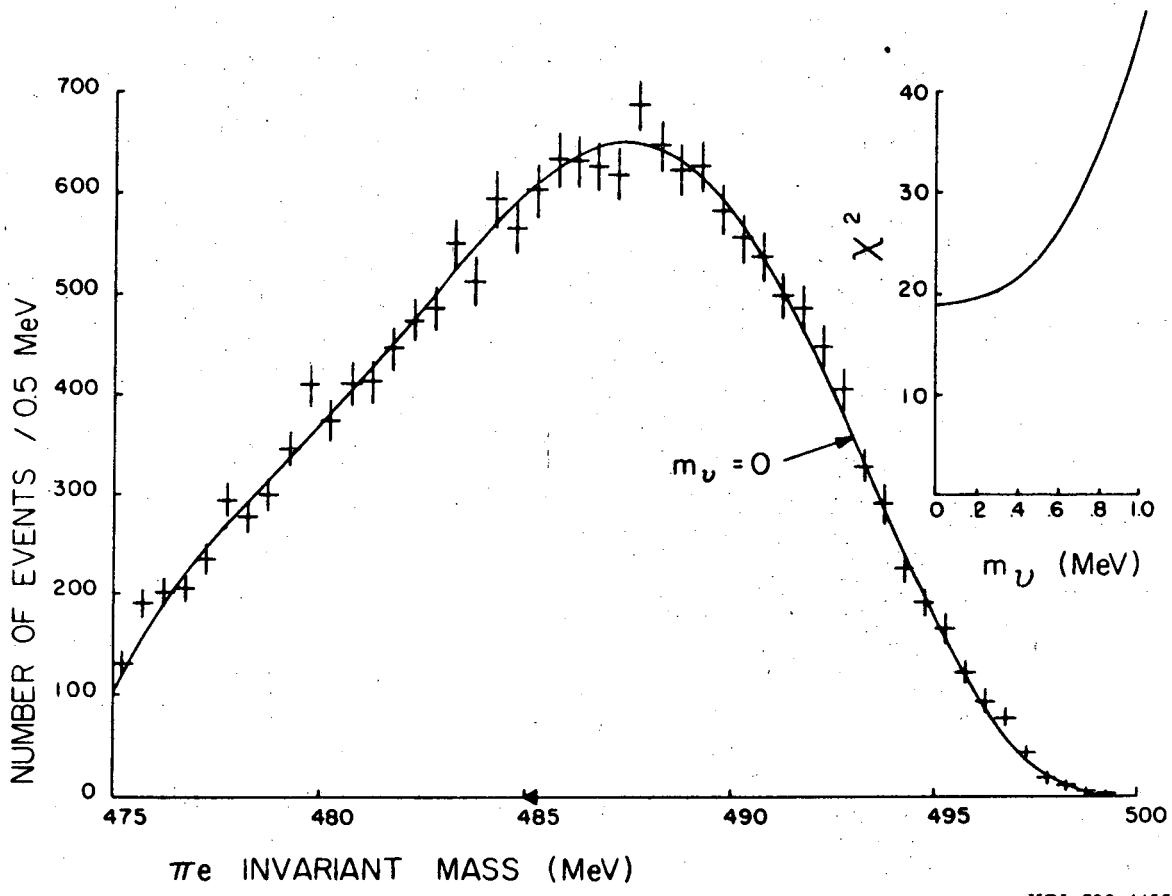
XBL 723-576

Fig. 2



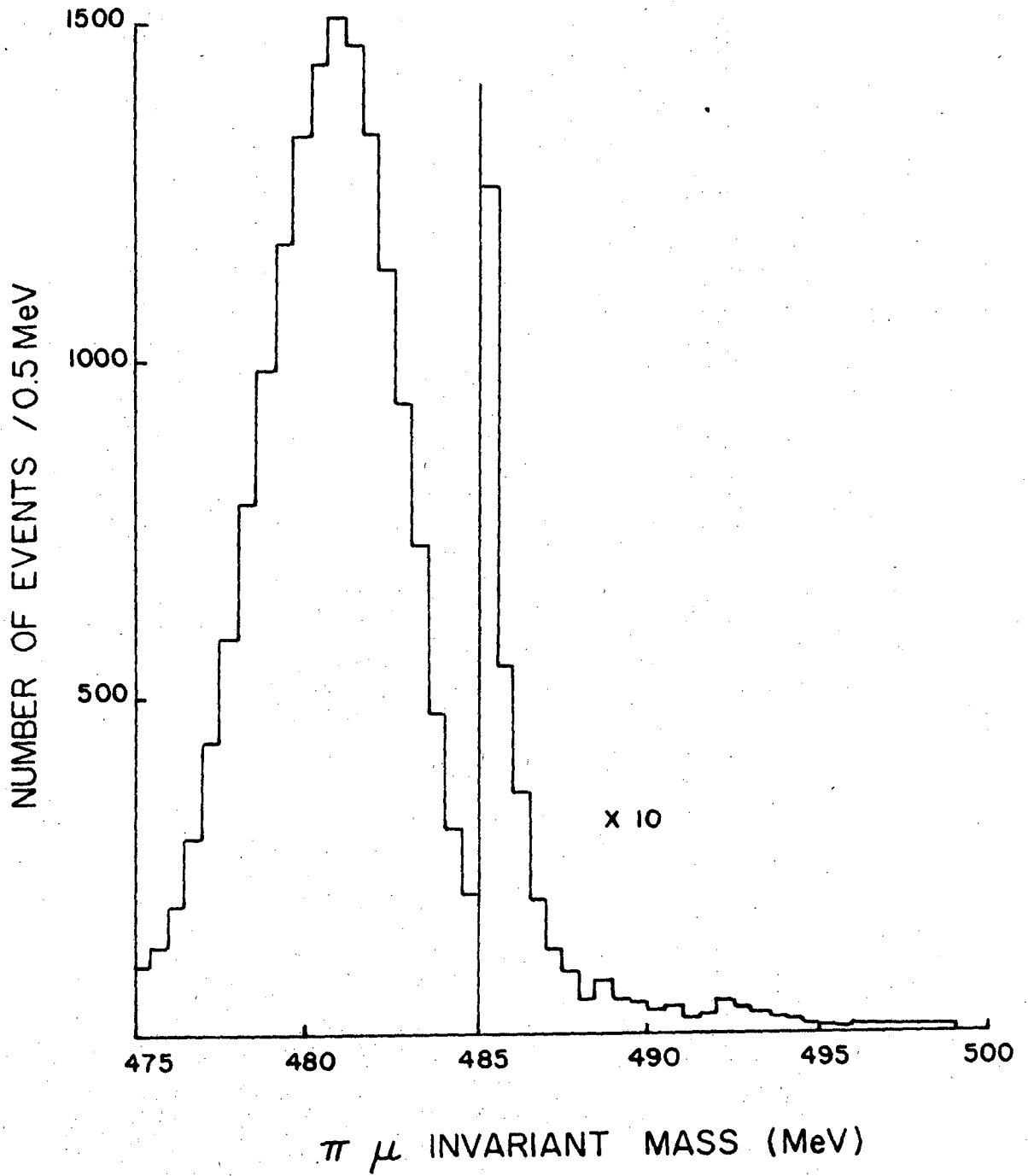
XBL 723-577

Fig. 3.



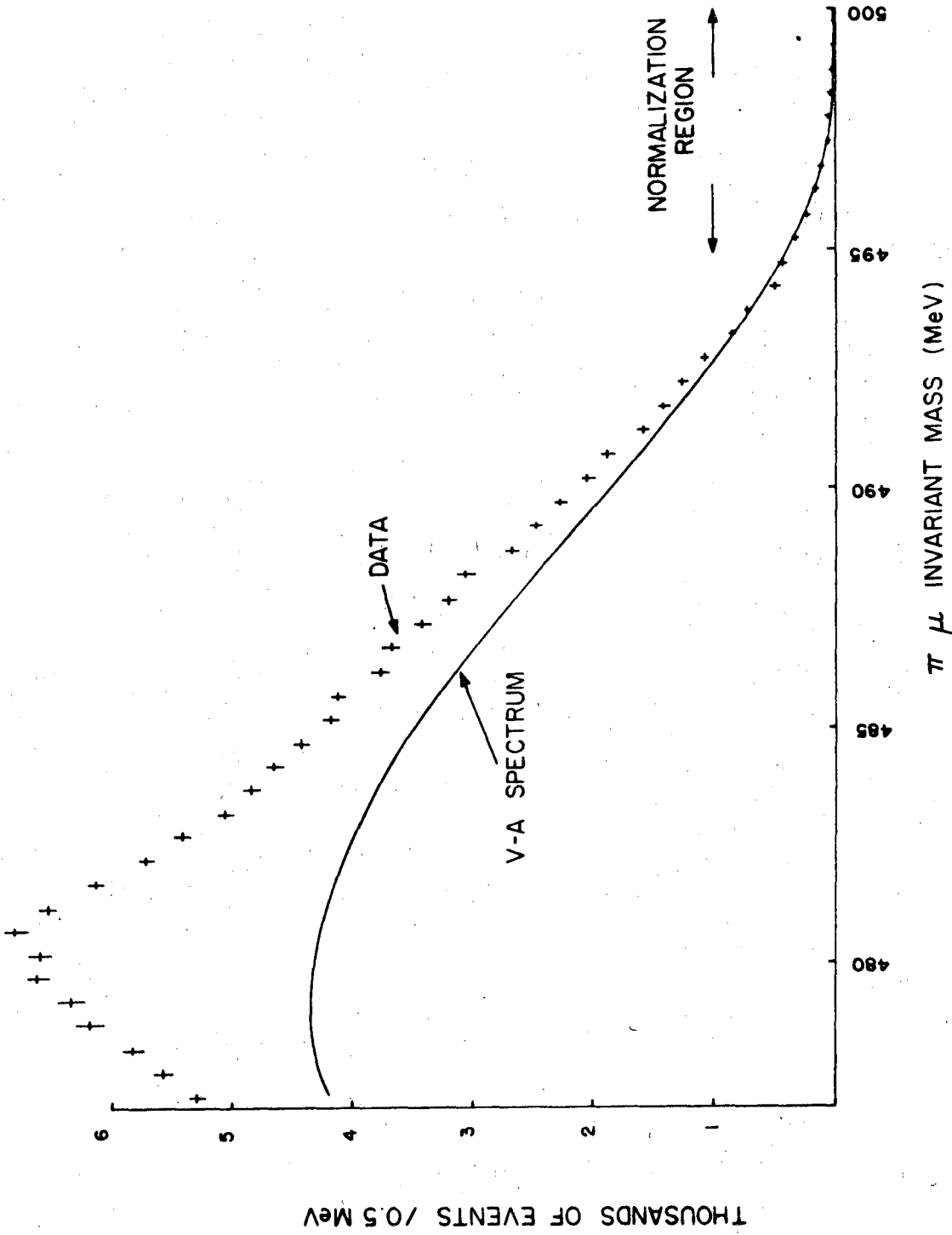
XBL 738-1155

Fig. 4



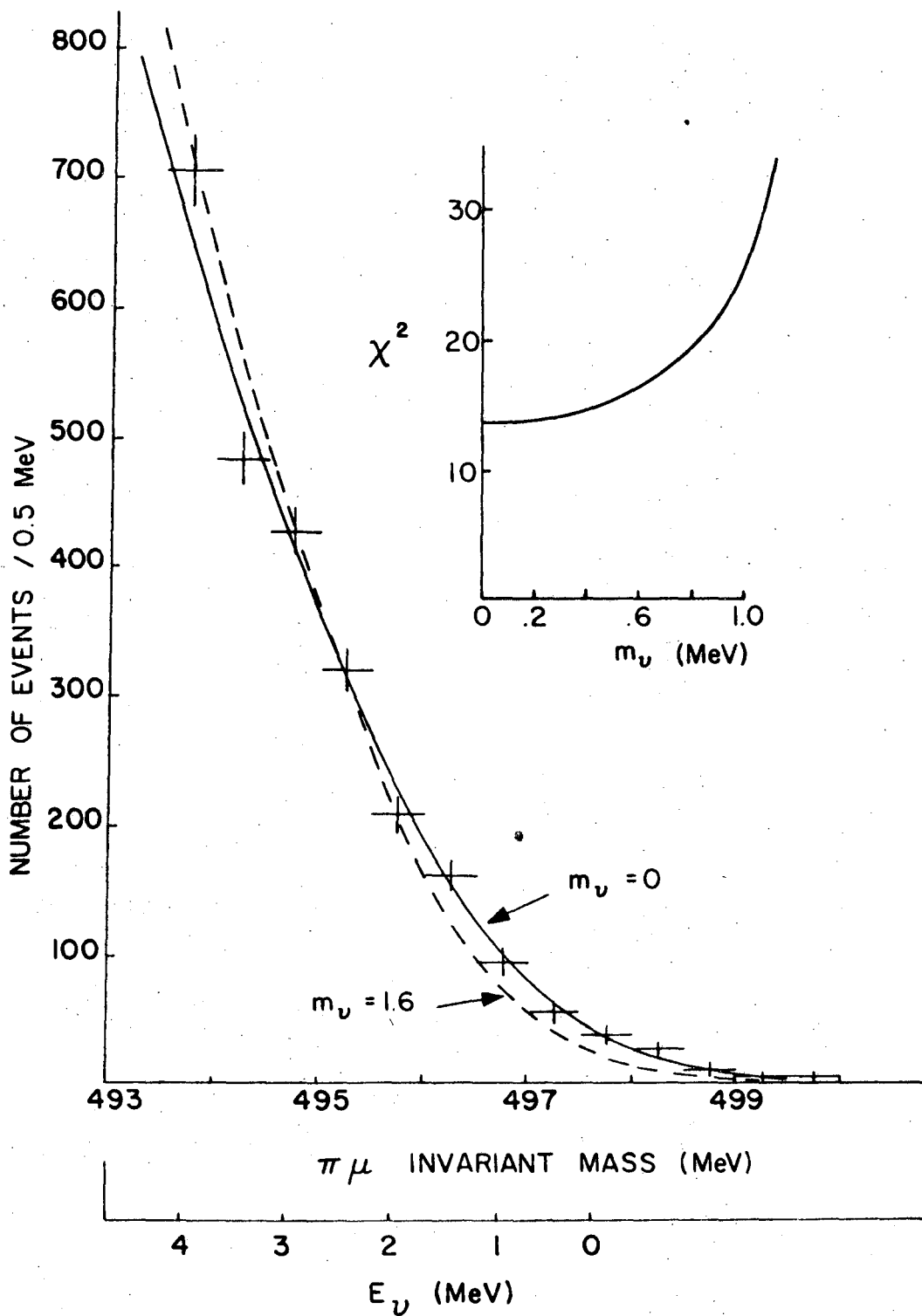
XBL 723-579

Fig. 5



XBL 723-581

Fig. 6



XBL 723-580

Fig. 7

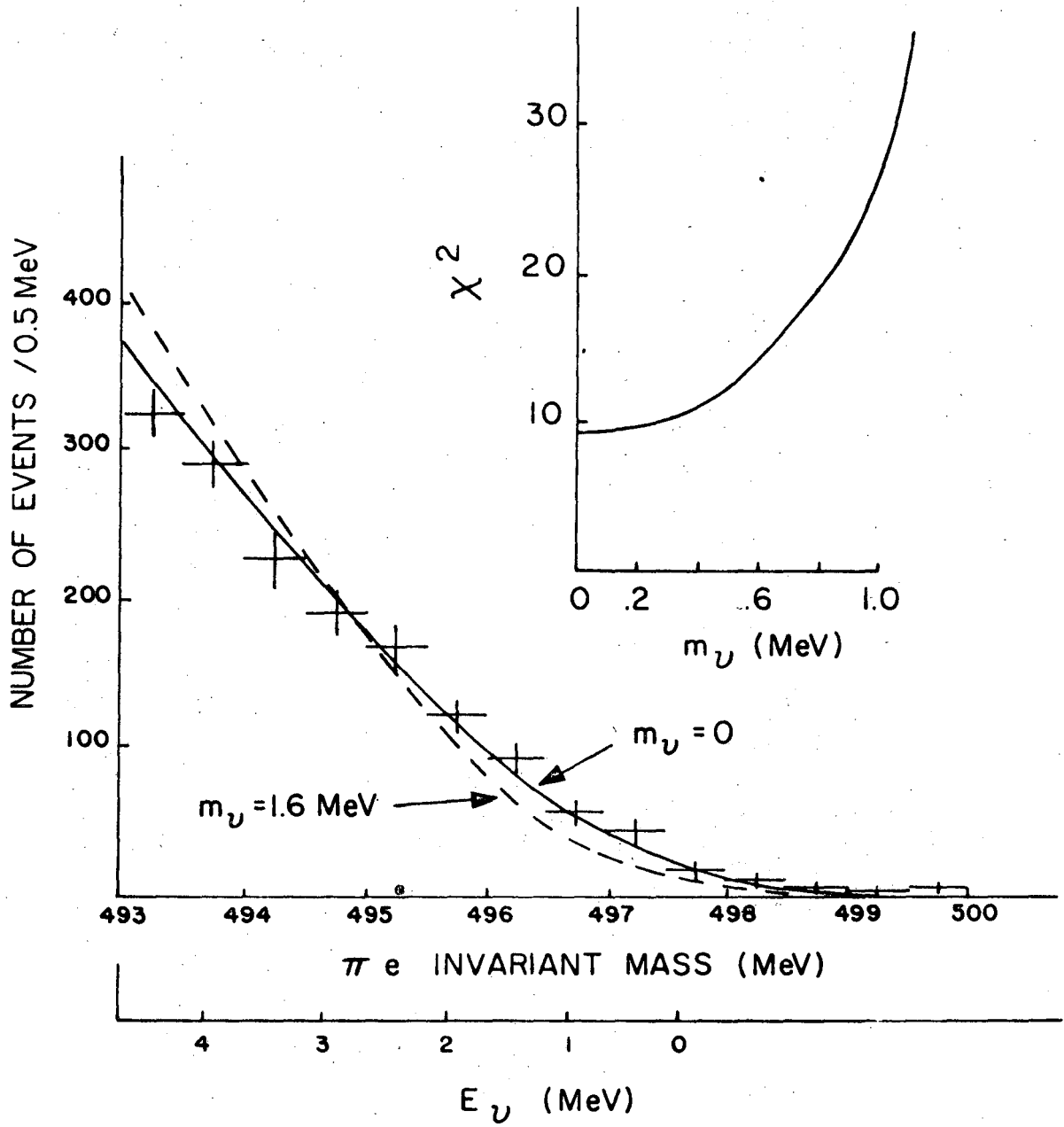


Fig. 8

XBL 723-578

LEGAL NOTICE

This report was prepared as an account of work sponsored by the United States Government. Neither the United States nor the United States Atomic Energy Commission, nor any of their employees, nor any of their contractors, subcontractors, or their employees, makes any warranty, express or implied, or assumes any legal liability or responsibility for the accuracy, completeness or usefulness of any information, apparatus, product or process disclosed, or represents that its use would not infringe privately owned rights.

TECHNICAL INFORMATION DIVISION
LAWRENCE BERKELEY LABORATORY
UNIVERSITY OF CALIFORNIA
BERKELEY, CALIFORNIA 94720